NMR Evidence for a Two-Step Phase Separation in $Nd_{1.85}Ce_{0.15}CuO_{4-\delta}$

O. N. Bakharev,[1] I. M. Abu-Shiekah,[1] H. B. Brom,[1] A. A. Nugroho,[2,*] I. P. McCulloch,[3] and J. Zaanen[3]

[1]*Kamerlingh Onnes Laboratory, Leiden University, POB 9504, 2300 RA Leiden, The Netherlands*
[2]*Van der Waals-Zeeman Institute, University of Amsterdam, 1018 XE Amsterdam, The Netherlands*
[3]*Instituut Lorentz for Theoretical Physics, Leiden University, POB 9506, 2300 RA Leiden, The Netherlands*

(Received 15 January 2004; published 15 July 2004)

By Cu NMR we studied the spin and charge structure in $Nd_{2-x}Ce_xCuO_{4-\delta}$. For $x = 0.15$, starting from a superconducting sample, the low temperature magnetic order in the sample reoxygenated under 1 bar oxygen at 900 °C reveals a peculiar modulation of the internal field, indicative of a phase characterized by large charge droplets ("blob" phase). By prolonged reoxygenation at 4 bars the blobs break up and the spin structure changes to that of an ordered antiferromagnet. We conclude that the superconductivity in the *n*-type systems competes with a genuine type I Mott-insulating state.

DOI: 10.1103/PhysRevLett.93.037002 PACS numbers: 74.72.Dn, 75.30.Ds, 75.40.Gb, 76.60.–k

At present an important issue in cuprate superconductivity is the nature of the electronic state(s) competing with the superconducting state (see [1,2] and references therein). In the hole doped cuprates evidence has been accumulating that at low dopings this competitor is a stripe phase [3]. It is believed that these stripe phases find their origin in the microscopic incompatibility between the metallic- and Mott-insulating states [4,5]. Stripes are *a priori* not a unique way of resolving this incompatibility. This was sharply formulated recently in terms of the analogy with superconductivity [6]; stripes can be viewed as the analogue of the type II superconductor while a type I behavior is also imaginable. In the latter the Mott insulator and the metal/superconductor are immiscible, and one expects a state characterized by droplets of the metal/superconductor in a Mott-insulating background. The electron doped (*n*-type) superconductors are microscopically [7] quite different from the hole doped ones, while macroscopic properties also seem distinct [8]. So far, no incommensurate spin fluctuations have been found by neutron scattering in this system [9–11], arguing against stripe phases. Instead, recently it was reported that field induced *commensurate* antiferromagnetism reemerges in the superconducting state in the presence of an Abrikosov vortex lattice [12], suggesting that the superconductivity competes with a conventional antiferromagnet.

Different from the *p*-type systems, the *n*-type systems stay insulating up to quite high dopings while the antiferromagnetism of half filling degrades quite slowly. In fact, Vajk *et al.* [10] showed that the behavior of this antiferromagnet can be understood in detail assuming a random dilution of the Heisenberg quantum antiferromagnet, suggesting that the individual carriers stay strongly bound to impurity sites. Is the field induced antiferromagnet of a similar kind? Using NMR we present here evidence that between the superconductor and the strong pinning phase there is yet another phase. By reoxygenating a superconducting $Nd_{2-x}Ce_xCuO_4$ (NCCO) sample with $x = 0.15$ up to the point that superconducting diamagnetism has disappeared, we have detected a phase in a very small oxygen-doping range located between the superconductor and the site diluted antiferromagnet. This phase is extremely sensitive to further oxygenation. Approximately one oxygen atom per 100 [13] unit cells suffices to destroy this phase, allowing a site-dilution antiferromagnet to take over. With NMR one can measure the *amplitude* distribution of the magnetic moments. These show a double-peak distribution in this special phase. Extensive Monte Carlo (MC) simulations on a representative model show that such a distribution only arises in either a stripe phase or a situation where *large* droplets are formed. Since the neutron scattering appears to rule out the former, we conclude that the superconductivity in the *n*-type systems competes with a genuine type I Mott-insulating state [6].

Experimental.—The experiments were performed on single crystals with $x = 0.15$, 0.12, and 0.08. For $x = 0.15$ the oxygen reduced sample (NCCO*p*) had a superconducting transition temperature of $T_c = 21$ K. Half of the crystal ($2 \times 1 \times 0.2$ mm) was reoxygenated in air at 900 °C until no superconductivity could be detected in the SQUID-susceptibility measurement (sample NCCO1). After performing the full set of NMR measurements, the same sample was oxygenated further under 4 bars of oxygen at 850 °C for 20 h (sample NCCO2), and NMR scanned again. Sample preparation and characterization are described elsewhere [14]. The Cu NMR spectra were obtained with conventional phase coherent pulsed NMR between 4 and 350 K by sweeping the magnetic field at various constant frequencies. The NMR line shift was determined by using a gyromagnetic ratio of 1.1285 MHz/kOe for ^{63}Cu and K = 0.238% of metallic Cu as a reference.

The Cu NMR spectra were studied for two orientations ($B_{\mathrm{appl}}||c$ and $B_{\mathrm{appl}}||ab$) of the crystals with respect to applied external magnetic field B_{appl}. An example for $x = 0.15$ with $B_{\mathrm{appl}}||c$ is shown in Fig. 1(a) at high temperature

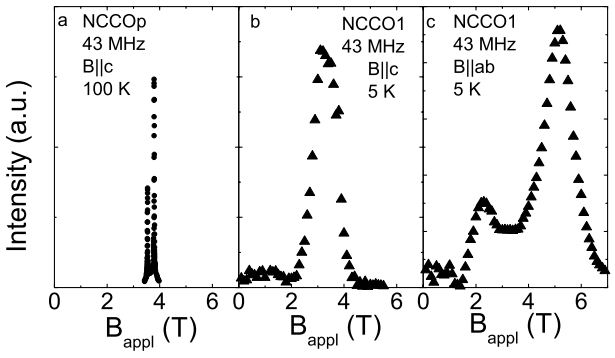

FIG. 1. Cu NMR spectra for $x = 0.15$ in NCCOp (for comparison scaled down from 78 to 43 MHz) at 100 K (at this temperature the spectra for NCCO1 and NCCO2 are identical to that of NCCOp) and NCCO1 at 5 K. The broadening and shifts at low temperature are clearly visible.

(100 K). The two narrow lines correspond to the central transitions of the two copper isotopes ^{63}Cu and ^{65}Cu and are superposed on a relatively broad background that likely originates from quadrupole satellites with small quadrupole frequencies. For characterization of the samples, we measured the T dependencies of the normalized product of the line intensity (I) (corrected for T_2 effects) and T, the NMR line shift ^{63}K, and the fundamental relaxation probability W_1 [15–18]. Here we concentrate on the low temperature field profiles on the Cu sites only; the internal field effects are so large that the role of the Nd moments can be neglected.

Analysis of the low temperature profiles.—In the presence of the static hyperfine magnetic field $B_{\rm hf}$ on the copper nuclei produced by ordered Cu^{2+} spins, one should observe two Cu NMR lines at $B = [B_{\rm appl}^2 + B_{\rm hf}^2 + 2B_{\rm appl}B_{\rm hf}\cos\alpha]^{0.5}$, where α is the angle between the directions of $B_{\rm appl}$ and $B_{\rm hf}$. It is known from neutron scattering experiments on $Nd_{1.85}Ce_{0.15}CuO_4$ [9] that the Cu^{2+} spins are ordered antiferromagnetically in the ab plane. Therefore, for $B_{\rm appl}||c$ ($\alpha = 90°$) only one Cu NMR resonance is expected at a lower value than the field calculated from the gyromagnetic ratio, B_0. For those nuclei, where for some reason the internal field is canceled, the resonance is unshifted. The Cu NMR spectra recorded for $B_{\rm appl}||c$ for $x = 0.08$, 0.13, and 0.15 can indeed be qualitatively explained in this way: for $x = 0.15$ [see Fig. 1(b)], part of the nuclei mainly feel the external field [resonate at the fields of Fig. 1(a)] and the remainder experiences an internal field in addition. At lower doping the line shifts are larger. The spectra for $B_{\rm appl}||ab$ [see Fig. 1(c)] seem to be composed out of at least two lines of different intensities. This difference is not due to T_2 or different $\pi/2$ conditions, because these are similar for both peaks [$T_2^{-1} = 23(1) \times 10^3\ {\rm s}^{-1}$ and $\pi/2 = 2\ \mu$s].

For a quantitative analysis, the low-temperature copper NMR spectra of NCCO1 at 5 K were simulated by exact diagonalization of the nuclear spin Hamiltonian $\mathcal{H}$ with effective spin $I = 1/2$ (the quadrupolar interaction is weak compared to the magnetic interaction) for both isotopes ^{63}Cu and ^{65}Cu. For $B \parallel c$, $\mathcal{H}$ can be written as $\mathcal{H} = \gamma\hbar B_{\rm appl} I_z + \gamma\hbar B_{\rm hf}[I_x\cos\varphi + I_y\sin\varphi] + \gamma\hbar B_1 I_x$, where the z direction is along the crystallographic c axis and φ is the angle between $B_{\rm hf}$ and the rf field B_1 (along the x axis); for $B \perp c$, I_z has to be replaced by I_y. $B_{\rm appl} \perp B_1$ in all experiments and the antiferromagnetic (AFM) coupled electron spins are assumed to be always in the (a, b) plane. The amplitude distribution of the internal field $P(B_{\rm hf})$ was obtained via Monte Carlo optimization to reproduce the data for $B \parallel c$ [see Fig. 2(a)]. Analysis of the $B \perp c$ data [Fig. 1(c)] with this pure in-plane AFM spin model indicates that the alignment of the electron spins is rather disordered in the (a, b) plane and, on average, shows a field induced canting of some 20°, which does not influence significantly the distribution $P(B_{\rm hf})$ in Fig. 2(a). In the $x = 0.12$, 0.08 samples the computations give a single peak at a field ~3 T, consistent with a simple commensurate antiferromagnet. However, in the slightly oxygenated $x = 0.15$ sample this spin-amplitude distribution is quite structured: the peak at 2.4 T (corresponding with a reduced moment of $\sim 0.14\mu_B$) is asymmetric, showing a slow decrease on the smaller moment side, while a second peak at the vanishing internal field corresponds with sites where the internal fields have completely disappeared.

Interpretation.—If the internal-field distribution would arise from a stripelike spin structure with wave vector k_x, we would have $P(B) = d(k_x x)/dB$ and hence $x \propto \int_0^{B/B_{\rm max}} P(B)\, dB$. Using the experimental outcome for $P(B_{\rm hf})$ the integration leads to the 1D wave depicted in Fig. 2(b); note that, because the Cu nuclei that experience

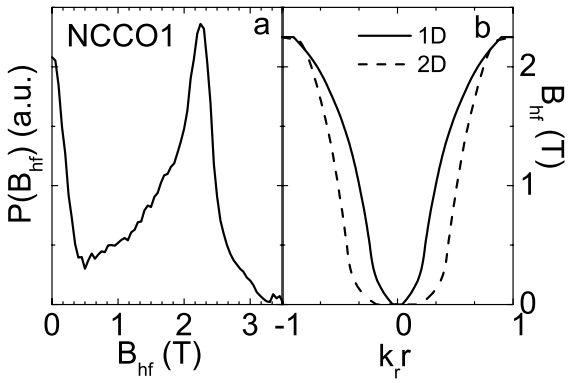

FIG. 2. (a) Amplitude distribution of the internal field for NCCO1 at 5 K. The solid line gives the profile of the hyperfine field, as deduced from $B \parallel c$. From the data for $B \perp c$ the antiferromagnetic alignment of the electron spins in the (a, b) plane appears to be strongly disordered (see text). (b) Simple reconstruction of the internal field distribution for a one- and two-dimensional spin structure. In 1D the radial coordinate r and (incommensurate) wave vector k_r have to be read as x and k_x. In 2D cylindrical symmetry is assumed.

B_{hf} have regular lattice positions, the wave vector needs to be incommensurate to realize such a field distribution at the Cu sites. The peak of $P(B_{\mathrm{hf}})$ at zero internal field in Fig. 2(a) then corresponds with the nodes. However, the field profile for a radially symmetric two-dimensional spin profile can be generated similarly via $(k_r r)^2 \propto \int_0^{B/B_{\max}} P(B)\, dB$ and is given in the same figure. These simple calculations are meant to show only that both stripelike structures (comparable to the 1D case) and charge blobs (2D case) are compatible with the experimental data. Furthermore, the needed zero field region in 2D is larger than in 1D (because of the transferred hyperfine interaction, the size of the blobs with zero spin exceeds the zero field region).

The size enters into the problem even stronger because of the specific form of the Hamiltonian. The internal field has not only an on-site contribution A, but also the transferred hyperfine interaction $B \approx A/4$, which gives a field of opposite sign, and hence in a droplet a nonzero field is generated on zero-spin sites (in a stripe configuration zero field states are easier to generate because it is an antidomain boundary). To make this case more persuasive we performed Monte Carlo simulations on a classical model designed to interpolate smoothly between stripelike and dropletlike ground state textures [19]. This is a classical, spin-full lattice gas model, which is similar to the model introduced by Stojković *et al.* [20]. It builds in the quantum-physical ingredient that electrons or holes ["charge," $\sim(1 - n_i)$] cause antiphase boundaries in the spin system by a "charge mediated" exchange interaction [21] coupling the spins antiferromagnetically across the charge, $H_{\mathrm{spin}} = J\sum_{x,y} S_{x,y}(S_{x,y+1} + S_{x+1,y}) + J_1 \sum_{x,y} S_{x,y}[(1 - n_{x,y+1})S_{x,y+2} + (1 - n_{x+1,y})S_{x+2,y}]$ with $J, J_1 \geq 0$. The frustration in the spin system is released by the formation of charged domain walls. The frustrated phase separation motive is built in by balancing the spin-mediated attractive charge-charge interactions with a repulsive $1/r$ Coulomb interaction of strength Q between the charges, which we cut off at ten sites (beyond the interstripe distance) for reasons of numerical efficiency [22]. We take an XY spin system, and the spin-orientational disorder is built in by a spin pinning potential, breaking the ground-state degeneracy by choosing a direction (up to spin reflection) for the antiferromagnetic background, as well as providing an inhomogeneous charge potential. It has the form $H_{\mathrm{Pot}} = -V_S|\sum_{x,y} S_{x,y} P_{x,y}|$, where $P_{x,y} = \sum_{x',y'} A_{x',y'} e^{i\Theta_{x',y'}} \times \exp[-\sqrt{(x - x')^2 + (y - y')^2}/R]$ with R the correlation length over which the antiferromagnetic background is allowed to rotate. The angle $\Theta_{x',y'}$ is chosen randomly with a uniform distribution and amplitude $A_{x',y'} = \mathrm{random}[0, 1]$. Finally we also incorporate a quenched disorder potential acting on the charge in the form of $V_C = \mathrm{random}[0, 1]$.

Despite its simplicity, this simple model is capable of generating quite complex ground states, ranging from highly disordered droplet patterns ($J_1 \to 0$) to very orderly stripe patterns $J_1, J \gg Q, V_S$. In the simulations we used small but finite temperatures and thermal annealing, mimicking the effects of quantum fluctuations in smearing the sharp textures [23] in this classical model. Two typical outcomes are illustrated in Figs. 3 and 4. We have extensively scanned the parameter space of this model. Invariably, we find that a double peak structure is easily associated with stripelike patterns [Fig. 3(b)], but these configurations invariably lead to incommensurate scattering amplitudes, which are not observed experimentally.

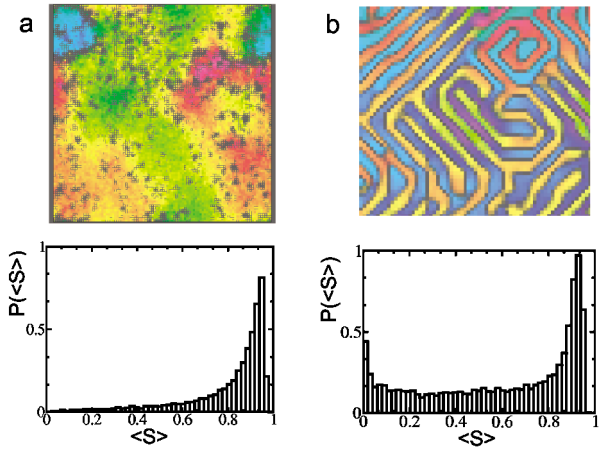

FIG. 3 (color). A 2D map of the blob (a) and stripe (b) results from thermalized averaged MC simulations, obtained with the Hamiltonian discussed in the text. The spin-orientational disorder in the (a, b) plane is represented by a difference in color (complementary colors correspond to opposite aligned spins), while the color intensity corresponds to the spin value. The spin-zero regions (black), as also seen in experiment, are found in the stripe simulations, but are almost absent for small blobs. The parameters for the blob and stripe panels are ($J = 1$, $V_C = 0$): $J_1 = 0.2$, $Q = 0.2$, $V_S = 0.2$, $R = 10$, $T = 0.4$ and $J_1 = 1$, $Q = 0.4$, $V_S = 0.2$, $R = 10$ with $T = 0.3$.

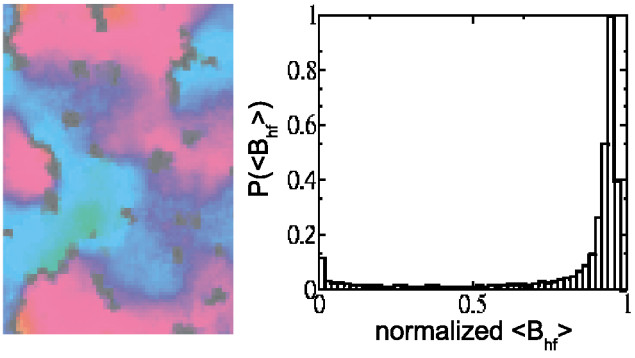

FIG. 4 (color). Blob results from the MC simulations: a thermalized result for larger blobs than in the previous figure. Only if blobs are sufficiently large, can zero field sites be generated in the presence of the transferred hyperfine interaction. For still larger blobs the zero field contribution further increases. Parameter values are $J = 1$, $T = 0.3$, $J_1 = 0$, $Q = 0.04$, $V_S = 0.2$ with $R = 10$ and $V_C = -1.5$.

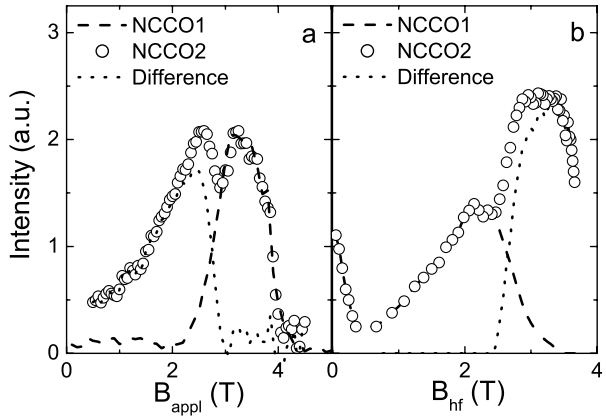

FIG. 5. Copper NMR spectra (the intensity in arbitrary units along the vertical axis is plotted against the magnetic field value in tesla) at 5 K for NCCO1 and NCCO2 (a). The lines in (b) are fits with an optimized internal field distribution (see text).

When droplets are formed instead, the zero-moment peak is always lacking for small droplets (Figs. 3 and 4). Only droplets of 2 nm or more (25 sites or larger) mimic the peculiarities of the NMR spectra. This adds confidence to our claim that the double peak structure in the local moment distribution is the NMR fingerprint signaling the presence of large charge blobs.

How can we reconcile our findings with the neutron scattering evidences favoring the site-diluted antiferromagnet? The NMR sample has a volume of 1 mm^3, much smaller than typical neutron targets, and we found the large droplet phase by almost continuously monitoring the disappearance of the superconducting state while the sample was oxygenated. Apparently, the large droplet phase in the NCCO1 sample is linked to the presence of a tiny amount of apical oxygens ($\delta \sim 0.005$ for NCCO1) [13]. The result for continuing the oxygenation of NCCO1 in 4 bars of oxygen as used in other studies [11] is given in Fig. 5. The data clearly show that in NCCO2 the phase of NCCO1 is suppressed in favor of a new phase [24]. Applying a similar analysis as before, we find that this new phase is characteristic of an antiferromagnet with an internal field of 3 T, the phase seen in the neutron data. Although it is hard to arrive at precise numbers, it seems that one extra oxygen per roughly 100 unit cells suffices to fracture the droplets and to favor a state where the charge carriers are strongly bound to impurities. As the superconductor, the large droplet insulating phase shows an extreme sensitivity to oxygen concentration explaining why this phase has been missed in the neutron scattering studies.

In summary, we have presented evidence demonstrating that the *n*-type cuprate superconductor is in a direct competition with a phase where the charge carriers form large droplets in a commensurate antiferromagnetic background. This phase is in turn extremely sensitive to the chemical conditions. Tiny amounts of excess oxygen suffice to destroy both superconductivity and the large droplet phase in favor of a phase where the charge carriers are strongly bound to the impurities.

We acknowledge fruitful discussions with Martin Greven (Stanford) and the financial support of FOM/NWO. Some of the numerical calculations were performed at the APAC National Facility via a grant from the Australian National University Supercomputer Time Allocation Committee.

*Present address: MSC, University of Groningen, Neijenborg 4, 9747 AG Groningen, The Netherlands.

[1] S. Sachdev, Rev. Mod. Phys. **75**, 913 (2003).
[2] S. A. Kivelson *et al.*, Rev. Mod. Phys. **75**, 1201 (2003).
[3] J. M. Tranquada *et al.*, Nature (London) **375**, 561 (1995).
[4] J. Zaanen and O. Gunnarsson, Phys. Rev. B **40**, 7391 (1989); M. Kato *et al.*, J. Phys. Soc. Jpn. **59**, 1047 (1990).
[5] V. J. Emery and S. A. Kivelson, Physica (Amsterdam) **209C**, 597 (1993).
[6] D. H. Lee and S. A. Kivelson, Phys. Rev. B **67**, 024506 (2003).
[7] J. Zaanen, G. A. Sawatzky, and J.W. Allen, Phys. Rev. Lett. **55**, 418 (1985).
[8] M. Imada, A. Fujimori, and Y. Tokura, Rev. Mod. Phys. **70**, 1039 (1998).
[9] K. Yamada *et al.*, J. Phys. Chem. Solids **60**, 1025 (1999).
[10] O. P. Vajk *et al.*, Science **295**, 1691 (2002).
[11] P. K. Mang *et al.*, cond-mat/0307093.
[12] H. J. Kang *et al.*, Nature (London) **423**, 522 (2003).
[13] Y. Onose *et al.*, Phys. Rev. Lett. **82**, 5120 (1999).
[14] A. A. Nugroho *et al.*, Phys. Rev. B **60**, 15 379 (1999).
[15] N. J. Curro *et al.*, Phys. Rev. Lett. **85**, 642 (2000).
[16] I. M. Abu-Shiekah, O. Bakharev, H. B. Brom, and J. Zaanen, Phys. Rev. Lett. **87**, 237201 (2001).
[17] A.W. Hunt, P. M. Singer, A. F. Cederström, and T. Imai, Phys. Rev. B **64**, 134525 (2001).
[18] Details of the NMR relaxation and line shift data will be published elsewhere and are available on request.
[19] K. Pijnenburg, Master's thesis, Leiden University, 1996.
[20] B. P. Stojković *et al.*, Phys. Rev. Lett. **82**, 4679 (1999).
[21] J. Zaanen, J. Phys. Chem. Solids **59**, 1769 (1998).
[22] Using cutoffs larger than the typical length scale of the highly structured solutions did not change the picture.
[23] J. Zaanen *et al.*, Philos. Mag. B **81**, 1485 (2001).
[24] Prolonged oxidation is expected to turn the crystal completely to the AFM phase; we decided to keep the sample in its present mixed state to allow further inspection.